


SCIENTIFIC REPORTS



OPEN

Pressure and high- T_C superconductivity in sulfur hydrides

Lev P. Gor'kov^{1,2} & Vladimir Z. Kresin³

Received: 02 February 2016

Accepted: 18 April 2016

Published: 11 May 2016

The paper discusses fundamentals of record- T_C superconductivity discovered under high pressure in sulfur hydride. The rapid increase of T_C with pressure in the vicinity of $P_{cr} \approx 123 \text{ GPa}$ is interpreted as the fingerprint of a first-order structural transition. Based on the cubic symmetry of the high- T_C phase, it is argued that the lower- T_C phase has a different periodicity, possibly related to an instability with a commensurate structural vector. In addition to the acoustic branches, the phonon spectrum of H_3S contains hydrogen modes with much higher frequencies. Because of the complex spectrum, usual methods of calculating T_C are here inapplicable. A modified approach is formulated and shown to provide realistic values for T_C and to determine the relative contributions of optical and acoustic branches. The isotope effect (change of T_C upon Deuterium for Hydrogen substitution) originates from high frequency phonons and differs in the two phases. The decrease of T_C following its maximum in the high- T_C phase is a sign of intermixing with pairing at hole-like pockets which arise in the energy spectrum of the cubic phase at the structural transition. On-pockets pairing leads to the appearance of a second gap and is remarkable for its non-adiabatic regime: hydrogen mode frequencies are comparable to the Fermi energy.

The search for high- T_C (“room”) superconductivity at high pressure was triggered by the suggestion¹ that one can expect high values of T_C in systems comprised of light atoms, including the metallic hydrogen. It is based on the fact that according to the BCS theory, the transition temperature is proportional to the frequency of phonons mediating the pairing. Half a century later, superconductivity at 190 K was claimed in sulfur hydrides under pressure $P > 150 \text{ GPa}$ ². Recently, $T_C \approx 203 \text{ K}$ was confirmed in H_3S formed in the decomposition of H_2S under pressure³.

The present work is mainly concerned with the peculiar pressure dependence of the superconducting transition temperature in sulfur hydride H_3S . According to recent data⁴, the value of $T_C \approx 100 \text{ K}$ at $P_{cr} \approx 123 \text{ GPa}$ sharply increases to $T_C \approx 200 \text{ K}$ at $P_{cr} \approx 150 \text{ GPa}$ as in a phase transition. In particular, once T_C reaches its maximum value $T_C \approx 200 \text{ K}$ at the onset of high- T_C phase it begins immediately to *decrease* with further increase in pressure^{3,4}.

We *assume* that the behavior of T_C in this pressure interval is a signature of a structural transition between phases with lower and higher T_C . Moreover, we argue that the first-order phase transition is the most credible concept for the near-doubling of T_C in the narrow experimental pressure interval $\Delta P \approx 25 \text{ GPa}$ and discuss the factors which account for such a significant increase in T_C . As concerns the microscopic mechanism which underlies the subsequent decrease in T_C , it is related to the coupling between the superconducting order parameters on hole-like pockets and on the main (“large”) part of the Fermi surface.

One should appreciate the challenges for theory in describing a material under high pressure. The common goal has been to establish stoichiometry, to prove the stability of the phases emerging at metallization, to identify transformations between the phases, to reconstruct the electronic bands and the phonons spectra, all from the *first principles*. Having obtained this information, one may attempt to evaluate the temperature T_C of the superconducting transition. Such an analysis was carried out in^{5–24}, including the successful prediction in^{5,6} of the H_3S -stoichiometry in agreement with the X-ray experiment⁴. At the same time, one finds inconsistencies between different theoretical publications, manifested especially sharply in the uncertainty of predictions of the specific phase transition pressure and for the symmetry of the phases.

According to the most publications, the mechanism of superconductivity in the high- T_C phase is phonon mediated electron-electron pairing on the “large” part of the Fermi surface. Based on calculated electron and phonon spectra, the transition temperature T_C has been deduced numerically with the use of the Migdal-Eliashberg

¹NHMFL, Florida State University, 1800 East Paul Dirac Drive, Tallahassee, Florida 32310, USA. ²L.D. Landau Institute for Theoretical Physics of the RAS, Chernogolovka 142432, Russia. ³Lawrence Berkeley Laboratory, University of California, 1 Cyclotron Road, Berkeley, CA 94720, USA. Correspondence and requests for materials should be addressed to L.P.G. (email: gorkov@magnet.fsu.edu)

(ME) equations^{25,26}. However, most of these algorithms were developed and optimized for ordinary metals. The applicability of the same methods to an analysis of the superconducting transition temperature in H₃S is scrutinized in the next Section. We introduce a new method for the evaluation of T_C based on generalization of the ME approach to the case of such a complex phonon spectra. To be more specific, the ME equations are rewritten to account for the fact that the phonon contributions from the optical and the acoustic branches have different characteristic frequencies and coupling constants.

The isotopic dependence of T_C (i.e., its change upon the substitution of deuterium for hydrogen) turns out to be different for the two sides of the phase transition, in agreement with the experiments^{3,4}. We conclude that the key role in the superconductivity of H₃S²⁻⁴ is played by high frequency hydrogen modes.

As was noted above, the mechanisms of superconductivity described in^{5-16,20,24} assert the prevailing role of the Cooper pairing on the large part of the Fermi surface. Standing apart is a scenario¹⁷⁻¹⁹ in which superconductivity in high- T_C phase is driven by the pairing on small hole-like pockets emerging at several spots of the Brillouin zone (BZ) via the Lifshitz 2.5-topological transition^{27,28}.

Hole-like pockets in the band structure of the high- T_C phase were theoretically exhibited in^{6,7,9,11,17,22}. The special role assigned to them in¹⁷ is owed to a van Hove (νH) singularity peak in the density of states (DOS) in close vicinity of the chemical potential, leading to a strong enhancement of the electron-phonon interactions. A peak in DOS is present in several band structure calculations^{6,11,12,17-19,22}, in²⁴ (see Fig. 4, Suppl. Mat.), but it lies at $0.15 \div 0.4$ eV below the chemical potential. The results below are in better agreement with the idea that the main contribution to pairing is due to the interactions at a large part of the Fermi surface, with pockets playing only a supportive role.

Experiment⁴ and the theory agree upon the body centered cubic lattice for the high- T_C phase of H₃S; then the electronic and phonons spectrum above $P = 200$ GPa are found to be consistent and are taken as the basis for the further analysis. Discrepancies among theoretical treatments at lower pressure will be discussed below.

Results

Transition temperature in high- T_C phase. The energy scale typical for the large part of the Fermi surface (broad bands) is a few eV. At $T = T_C$ the equation for the order parameter $\Delta(\omega_n)$ is:

$$\Delta(\omega_n)Z = -T \sum_m \int d\xi \int d\omega \frac{\alpha^2(\omega)F(\omega)}{\omega} D(\omega, \omega_n - \omega_m) \times \frac{\Delta(\omega_m)}{\omega_m^2 + \xi^2} \quad (1)$$

Here $\Delta(\omega_m)/(\omega_m^2 + \xi^2)$ is the pairing Greens function²⁹; $D(\omega, \omega_n - \omega_m) = -\omega^2/[(\omega_n - \omega_m)^2 + \omega^2]$ is the phonon propagator; ω is the phonon frequency, ξ is the electron energy referred to the chemical potential, $\omega_n = (2n + 1)\pi T$. We are employing the method of thermodynamic Green's functions; see, e.g.,³⁰. The function $\alpha^2(\omega)F(\omega)$ is a well-known quantity determining the strength of the electron-phonon interaction (see, e.g.^{31,32}), $F(\omega)$ is the phonon density of states, $Z \approx 1 + \lambda$ in (1) stands for the band mass renormalization. The coupling constant λ is defined by the expression:

$$\lambda = 2 \int [\alpha^2(\omega)F(\omega)/\omega] d\omega \quad (2)$$

It is essential that Eq. (1) does not explicitly contain the coupling constant λ . Indeed, it involves integration over the phonon frequency ω which enters not only in the factor $\alpha^2(\omega)F(\omega)$, but in the phonon propagator $D(\omega, \omega_n - \omega_m)$ which also depends on $\omega_n - \omega_m$.

It is apparent from Eqs. (1, 2) that the coupling constant can be factored out if Eq. (1) does not contain a phonon propagator function (e.g., $D \approx 1$ for the weak coupling case) or if the dependence of D on the frequency ω can be neglected.

In principle, the value of T_C can be calculated directly from the full non-linear equation for the order parameter $\Delta(\omega_n)$ (at $T < T_C$ one should substitute $\xi^2 \Rightarrow \xi^2 + \Delta^2(\omega_n)$ in Eq. (1)). Such a program was carried out in^{11,12,15,24} in the framework of the superconducting density functional theory (the calculation in²⁴ was extended beyond constant-DOS approximation and without treating the pseudopotential μ^* as an empirical parameter). The impact of anharmonicity was studied in¹⁵. The value of T_C was calculated from the non-linear equation for $\Delta(\omega_n)$ by iterations.

An important point to emphasize is the following. The analysis of usual superconductors is based on the concept of a coupling constant, λ which makes it possible to obtain an analytic expression for T_C . The fact of the matter is that in common metals the function $\alpha^2(\omega)F(\omega)$ is characterized by a peak in the phonon density of states (DOS) $F(\omega)$ (see, e.g.^{31,32}). This peak corresponds to the short-wavelength part of the spectrum where the mode dispersion $\omega(\vec{q})$ is weak. This permits the replacement of $\omega(\vec{q})$ in the phonon propagator by its average value $\bar{\omega}^{32-34}$ (the latter taken either as $\bar{\omega} = \langle \omega^2 \rangle^{1/2}$, see, e.g.³³, or $\bar{\omega} = \langle \omega_{\log} \rangle$, which is close to $\langle \omega^2 \rangle^{1/2}$, see^{35,36}).

The principal cause for concern about the applicability of the same scheme to H₃S is that the phonon spectrum of sulfur hydride is complex and consists of the well-separated acoustic and optical branches; the phonon DOS contains several peaks. As a consequence, introducing a coupling constant λ and the characteristic frequency $\bar{\omega}$ should be done with considerable care.

Our approach is to separate the phonon spectrum in the two regions of the optical and acoustic phonons and for each of them to introduce their respective average frequencies $\bar{\omega}_{opt}$ and $\bar{\omega}_{ac}$ and the coupling constants λ_{opt} and λ_{ac} . Such separation allows us to compare the relative contributions of the optical and acoustic phonons. Then Eq. (1) takes the following form:

$$\Delta(\omega_n)Z = T_C \sum_m \int d\xi [(\lambda_{opt} - \mu^*)D(\tilde{\omega}_{opt}, \omega_n - \omega_m) + \lambda_{ac}D(\tilde{\omega}_{ac}, \omega_n - \omega_m)]\Delta(\omega_m)/(\omega_m^2 + \xi^2). \quad (3)$$

Here $\lambda_i = \int_i d\omega \alpha^2(\omega)F(\omega)/\omega$; $\tilde{\omega}_i = \langle \omega^2 \rangle^{1/2}$; $\langle \omega^2 \rangle = (2/\lambda_i) \int_i d\omega \alpha^2(\omega)F(\omega)\omega$; $i \equiv \{opt., ac.\}$. The critical temperature can be calculated with the use of Eq. (3).

Let us assume that in high- T_C phase $\lambda_{opt} \gg \lambda_{ac}$. We also suppose that $\lambda_{opt} \lesssim 1.5$. As will be shown below, these conditions are indeed satisfied.

Let us write T_C as $T_C = T_C^0 + \Delta T_C^{ac}$ and assume that $\Delta T_C^{ac} \ll T_C^0$. As the first step, let us neglect the contribution of the acoustic phonons. The value of T_C^0 can be obtained from Eq. (3) keeping only the first term on the right-hand side of Eq. (3). As the solution for T_C^0 , one can use either the McMillan-Dynes expression^{37,38} which is valid for $\lambda_{opt} \lesssim 1.5$, or the close expression, obtained analytically in³⁴:

$$T_C^0 \approx \frac{\tilde{\omega}_{opt}}{1.2} \exp \left[-\frac{1.04(1 + \lambda_{opt})}{\lambda_{opt} - \mu^*(1 + 0.62\lambda_{opt})} \right]. \quad (4)$$

To find a correction ΔT_C^{ac} due to the acoustic phonons contribution, consider the full Eq. (3). Substituting the total $T_C = T_C^0 + \Delta T_C^{ac}$ in the first term on its right-hand side and T_C^0 in the second term, we obtain after a calculation (see Supplemental Materials A):

$$\frac{\Delta T_C}{T_C^0} \approx 2 \frac{\lambda_{ac}}{\lambda_{opt} - \mu^*} \times \frac{\rho^2}{\rho^2 + 1}. \quad (5)$$

Here $\rho = \tilde{\omega}_{ac}/\pi T_C^0$. These results can be used to evaluate T_C for the cubic high- T_C phase.

The values of the coupling constants and μ^* (usually $\mu^* \approx 0.1 \div 0.15$) for ordinary superconductors can be determined from tunneling spectroscopy measurements (see, e.g.³²); tunneling spectroscopy also has been used to study the effect of pressure³⁹. Since such measurements have not been performed for sulfur hydride, we deduce the coupling constants λ_{opt} and λ_{ac} from several theoretical calculations of $\alpha^2(\omega)F(\omega)$. Although the theoretical results differ somewhat, they are relatively close. According to^{6,13}, we estimate $\lambda_{opt} \approx 1.5$ and $\lambda_{ac} \approx 0.5$; these values consistent with the above approximations. Using these coupling constants and taking for $\tilde{\omega}_{opt}$ and $\tilde{\omega}_{ac}$ the values $\tilde{\omega}_{opt} \approx 1700 K$ and $\tilde{\omega}_{ac} \approx 450 K$ ($\mu^* \approx 0.14$ which is close to that for usual superconductors and was also calculated in¹¹), we obtain $T_C^0 \approx 170 K$ and $\Delta T_C^{ac} \approx 45 K$, so that in total $T_C \approx 215 K$, in quite good agreement with $T_C \approx 203 K$ observed in⁴. The main contribution comes from the optical phonons, this confirms the self-consistency of our approach.

The fact that the coupling constant λ_{opt} in the cubic phase is so large is a key ingredient underlying the observed high $T_C \approx 203 K$. Qualitatively, this is due to the ability of sulfur to retain several hydrogen atoms in its proximity, that is, to the presence of many light ligands near the S atoms.

The method proposed above can be of relevance for other materials as well. A promising example is calcium hydride⁴⁰. The corresponding analysis with the use of our approach will be described elsewhere.

The papers cited above calculate T_C without dividing the phonon spectrum in two parts. As discussed above, the approximation of defining an average $\tilde{\omega} = \langle \omega_{log} \rangle$ for the entire spectrum is hard to justify. Furthermore, the McMillan-Dynes equation used in these references to calculate T_C is not valid for total coupling constant as large as those obtained in³³⁻³⁵.

Within our approach, on the other hand, λ_{opt} is within the range where Eq. (4) is applicable. As for Eq. (3), it allows us to evaluate the relative contribution of the optical and acoustic branches of the phonon spectrum to T_C : ~80% is due to the optical phonons and only ~20% is due to the acoustic part.

Isotope effect. The isotopic dependence of T_C (change upon the substitution of deuterium for hydrogen²⁻⁴) is of fundamental importance, since it proves (a) that the high T_C state is caused by the electron-phonon interaction and (b) that it is the high frequency hydrogen modes that determine the value of T_C . Indeed, the optical modes are mainly due to motion of hydrogen, whereas for the acoustic modes the participation of sulfur ion prevails. Therefore the magnitude of the isotope coefficient reflects indirectly the relative contributions of the each group (optical vs. acoustic) into the observed T_C .

For the cubic high- T_C phase the value of the isotope coefficient (in the harmonic approximation),

$$\alpha = -(M/T_C)(\partial T_C/\partial M)(\partial \tilde{\omega}_{opt}/\partial M) = 0.5(\tilde{\omega}_{opt}/T_C)(\partial T_C/\partial \tilde{\omega}_{opt}), \quad (6)$$

can be evaluated from Eqs (4, 5). After a calculation we obtain:

$$\alpha \approx \frac{1}{2} \left[1 - 4 \frac{\lambda_{ac}}{\lambda_{opt}} \times \frac{\rho^2}{(\rho^2 + 1)^2} \right]. \quad (7)$$

Here $\rho = \tilde{\omega}_{ac}/\pi T_C^0$. With $\lambda_{opt} \approx 1.5$, $\lambda_{ac} \approx 0.5$, $\tilde{\omega}_{ac} \approx 450 K$ (see the Supplemental Material A) we obtain $\alpha \approx 0.35$ in good agreement with⁴. Note that the value of α can be affected by anharmonicity^{12,13} and by the dependence of μ^* on $\tilde{\omega}_{opt}$, although the last contribution is of the order of $(\mu^*/\lambda_{opt})^2$ and is small.

It is noteworthy that the isotope coefficient in the low- T_C phase is different. Indeed, according to⁶, the coupling constants for this phase are $\lambda_{opt} \approx \lambda_{ac} \approx 1$. These values reflect a larger relative contribution of the acoustic modes. In this case $T_C < \tilde{\omega}_{ac} \ll \tilde{\omega}_{opt}$ and within the usual BCS logarithmic approximation one can obtain:

$$T_C \approx const \times (\tilde{\omega}_{opt})^{\lambda_{opt}/\lambda_T} (\tilde{\omega}_{ac})^{\lambda_{ac}/\lambda_T} \exp[-(1 + \lambda_T)/(\lambda_T - \mu^*)]. \quad (8)$$

Here $\lambda_T = \lambda_{ac} + \lambda_{opt}$; $Z \approx (1 + \lambda_T)$ is included into the exponent^{33,37}.

With $\tilde{\omega}_{opt} \approx 105 \text{ meV}$ and $\tilde{\omega}_{ac} \approx 26 \text{ meV}$ for the low- T_C phase (see⁶) we obtain $T_C \approx 120 \text{ K}$.

From Eqs. (6, 8) one finds $\alpha \approx 0.25$, which is noticeable smaller than for the high- T_C phase. Experimentally⁴ the impact of the isotopic substitution in the region of smaller T_C is weaker than in the high- T_C phase, in agreement with our analysis.

Smaller α reflects the larger role played by the optical phonons in the *cubic* phase, resulting in its higher T_C .

Phase sequence. The phase diagram of sulfur hydride has been studied with *ab initio* calculations^{5–17}. According to²³, in the low pressure regime there is a microscopic mixture of phases. The smallness of the enthalpy for stoichiometric H_2S - H_3S boundaries may result in the formation of metastable alloy-like structures containing both components.

A few structures have been identified as the most energetically stable phases. According to⁶, below 100 GPa we are dealing with the *Cccm*-structure. On the other side, according to all the relevant publications, at pressures $P \geq 200 \text{ GPa}$ the system forms the body-centered cubic *Im* $\bar{3}m$ (*Im-3m*) lattice with one entity H_3S per unit cell. To emphasize, in this pressure range theoretical results^{5–17} for the electron and phonon spectra differ only in minor details.

At *intermediate* pressures first principle calculations disagree significantly regarding the critical pressure and the symmetry of the phase preceding the *Im-3m* one. According to⁶, the *Im-3m* phase gives way to the phase *R3m* below 180 GPa . Both in¹¹ and in⁶ the *Cccm* structure remains stable up to $P = 95 \text{ GPa}$.

For the interval $P = 95 \div 150 \text{ GPa}$ the thermodynamic phase is *R3m* (β -*Po*-type), see¹¹, but the *Im-3m* lattice sets in at the pressure $P = 150 \text{ GPa}$, instead of $\approx 180 \text{ GPa}$ in⁶. The results for the ground state are given in⁹ only for two pressures $P = 150 \text{ GPa}$ and $P = 200 \text{ GPa}$. Favorable at $P = 200 \text{ GPa}$ is the *Im-3m* structure, but the *R3m* phase prevails at $P = 150 \text{ GPa}$. The last result contradicts¹¹, but is in agreement with⁶.

Thermodynamics of the transition. The rapid growth of T_C in the pressure interval of 125 – 150 GPa ^{3,4} raises the question of whether this rapid T_C -variation is indeed due to a structural phase transition, and if this is the case then what are the two adjacent phases. The T_C data in Fig. 3c of paper⁴ is obtained both while increasing and decreasing the pressure point at the discontinuous transition, although the character of the transition cannot be deduced unambiguously only from the pressure dependence of T_C . As shown above, the accuracy of the *ab initio* calculations is insufficient to determine theoretically the precise value of the critical pressure for the transition between the low- T_C and high- T_C phases. One should note, however, for the purpose of determining the order of the transition between the two phases these uncertainties are less relevant than symmetry arguments. To cast the analysis in terms of the Landau theory of the symmetry phase transitions⁴¹, it is convenient to consider the phase transformations in the reverse order, that is, as a function of *decreasing* pressure.

According to^{11–13}, the transition into the *R3m* phase is driven by softening of the sulfur-hydrogen stretching mode. The cubic space group *Im-3m* (O_h^3) contains *inversion* as one of the symmetry elements. Space group #160 (*R3m*) belongs to the class C_{3v} for which *inversion* is absent. Hence, the second-order transition between the high- T_C *Im-3m* phase and the phase *R3m* does not contradict to the Landau theory⁴¹. Note that the notation *R3m* (β *Po*-type) used in¹¹ is for the same rhombohedral *R3m* phase as in^{12,13}.

This specific result¹³ may be sensitive to the calculation details; indeed, for the critical pressure P_{cr} one finds $P_{cr} = 150 \text{ GPa}$ in¹¹ vs. $P_{cr} = 103 \text{ GPa}$ ¹³. However, with the use of the group-theoretical symmetry analysis, we can prove *rigorously* that the list of the phonon modes available at the center of the Brillouin Zone (BZ) for the point group $O_h = T_d \times C_i$ is comprised of four *odd* three-dimensional irreducible representations (three vector representations F_{2u} and one F_{1u} ⁴²), so that *any* instability with the zero structural vector would result in the second order transition.

According to¹³, the “imaginary phonon frequencies” appear at several points of the BZ (in the harmonic approximation). Furthermore, to the best of the authors’ understanding, the *first principle* calculations^{11–13} never discussed softening of a phonon frequency $\omega(\vec{Q})$ due to its renormalization via the electron-phonon interactions (see^{23,43,44}), and we infer that instabilities with a non-zero structural vector in sulfur hydrides remain unexplored. We mean a structural transition with a change in periodicity or the usual charge density wave (CDW) transition (see in⁴⁵). Note that the problem of the CDW instability with a non-zero structural vector \vec{Q} was investigated long ago in transition-metal dichalcogenides with the *incommensurate* and *commensurate* CDW phases separated below the instability point by a first-order phase transition⁴⁶. (The *trigonal R3m* phase with three H_3S entities per unit cell suggested in³ is the example of the commensurate modulated phase).

As pointed out above, the abruptness of the T_C -variation^{3,4} testifies in favor of a first-order transition. To clarify the issue, X-rays measurements with higher resolution are required.

Fine bands structure and role of hole-like pockets. The fine structure of the electronic energy spectrum in the high- T_C phase consists of small hole-like pockets at several locations within the BZ, with the Fermi energy on the order $0.5 \text{ eV} \div 100 \text{ meV}$. As emphasized above, the presence of the pockets seems to be reliably established in the band calculations^{6,9,11,12} (see Fig. 6 in Suppl. to¹²)^{17–19}. In addition, tunneling experiments would be able to confirm the existence of small pockets by the observation of the two superconductivity gaps.

However, there is no agreement regarding the importance of the small pockets for superconductivity at the high temperature of $T_C \approx 203$ K in H_3S . Since the position of a van Hove singularity peak at the Fermi level appears uncertain, it is worth considering the possibility of superconductivity arising in a pocket without additional special assumptions.

Interaction of carriers on small pockets with high frequency phonons cannot be included into the scheme²⁶, as the Migdal parameter²⁵ ω_{opt}/E_F for the hydrogen modes is of the order of unity¹⁷. Leaving aside the vH-peak hypotheses¹⁷, the temperature T_C for the pairing on a pocket can be estimated in the weak-coupling approximation⁴⁷.

For simplicity, consider carriers on a single pocket with the Fermi energy E_F interacting with one acoustic mode with the frequency $\omega_{ac} \ll E_F$ and with one optical phonon with a frequency $\omega_{ac} \ll \omega_{opt}$ (ω_{opt} is of the order of E_F). Introduce the quantities $2\gamma_{ac}^2\nu(E_F) = \lambda_{ac}^{pocket}$ and $2\gamma_{opt}^2\nu(E_F) = \lambda_{opt}^{pocket}$; here γ_{opt} and γ_{ac} are the matrix elements of the electron-phonon interactions.

In conventional metals the dimensionless λ 's are usually between 1/2 and 1/4. The magnitudes of γ_{opt} and γ_{ac} can be assumed to be similar to those in ordinary metals. What makes λ_{ac}^{pocket} and λ_{opt}^{pocket} small in the present case is the differences in DOS compared to large Fermi surfaces; then the T_C value possible for hole-like pockets can be evaluated in the weak coupling limit.

The expression for the pairing T_C for a pocket has the form[cf. with Eq. (8)]:

$$T_C = const \times \tilde{\omega}_{ac} \exp[-1/\lambda_T^{pocket}] \times (\tilde{\omega}_{opt}/\tilde{\omega}_{ac})^\beta. \quad (9)$$

Here $\tilde{\omega}_{opt}$ is on the order of E_F and $\beta = \lambda_{opt}^{pocket}/(\lambda_T^{pocket}) \leq 1$. (See in the Supplemental Materials B). Estimating uncertainties in $DOS \propto m^* p_F$ and taking $\tilde{\omega}_{ac} \approx 50$ meV and $\omega_{opt}/\omega_{ac} \approx 3 \div 4$ in Eq. (6) one arrives at a T_C between one and a few tens Kelvin.

In the scenario¹⁷ a peak in DOS makes the coupling constants λ_{opt}^{pocket} and λ_{ac}^{pocket} in Eq. (6) large enough to account for the high temperature $T_C \approx 180 \div 200$ K in the cubic phase. The superconducting ordering emerges in the pocket, and induces an order parameter on the large part of the Fermi surface.

As emphasized above, we find this possibility unlikely. A temperature $T_C \approx 215$ K that was obtained above is close to the values estimated for T_C on the large Fermi surfaces in^{5-8,11-16}. In both cases the magnitude of the transition temperature is correct and there is no need for additional mechanisms. Besides, as mentioned above, peaks in DOS are usually located $0.17 \div 0.4$ eV below the chemical potential.

The above estimates for T_C in a pocket further confirm the prevailing role of the large part of the Fermi surfaces. We infer, together with^{5-8,11-16}, that the superconductivity of hybrid sulfur is driven by phonon-mediated pairing on the broad bands.

One should stress, in addition, that if a van Hove singularity in DOS were assumed to play a leading role, this would result in a change of the prefactor in Eq. (6): $\tilde{\omega}_{ac} \Rightarrow W$ where W is the width of the van Hove peak. However, being of the electronic origin the latter cannot depend on the ionic mass, in stark contradiction with the observed isotope effect²⁻⁴.

Origin of the T_C -maximum in high- T_C phase. The behavior of the temperature of the superconducting transition as a function of pressure is asymmetric with respect to its maximum $T_{C,max} \approx 203$ K in the high- T_C phase⁴. The rapid T_C decrease at $T < T_{C,max}$ appears consistent with the hypothesis of a *discontinuous* structural first-order transition at $P_{cr} \approx 123$ GPa. Additional light on the issue is shed by analyzing the subtle contribution of small pockets.

To describe the major features of the phenomenon, let us consider the two-band model. Then $\Delta(\omega_n)$ and $\Xi(\omega_n)$ are the two superconductivity order parameters of the pocket and of the broad band, respectively. Assuming that the two bands are weakly coupled, the superconductivity pairing on the pocket change T_C of the whole system only slightly.

Let us, for conciseness, consider only the contribution of the optical phonons. The linear equation for the parameter $\Xi(\omega_n)$ at $T = T_C$ can be written as follows (see in the Supplemental Materials C)

$$\{T_C - T_{C0}\}\Xi(\omega_n) = \pi \{\gamma_{12}^2 \gamma_{21}^2 / \gamma_{11}^2\} \nu_P(E_F) T_{C0} \sum_m |D_{opt}(\omega_n - \omega_m)| (1/|\omega_m|) \Xi(\omega_n) \quad (10)$$

In this equation $|D_{opt}(\omega_n - \omega_m)| = \omega_{opt}^2 / [(\omega_n - \omega_m)^2 + \omega_{opt}^2]$, and γ_{11} and γ_{12} are the matrix elements of the electron-phonon interaction on the large Fermi surface and for electron-phonon scattering between the large and the small Fermi surfaces, respectively ($\gamma_{12} \ll \gamma_{11}$). (The critical temperature $T_C > T_{C0}$).

The density of states on the large Fermi surface (LFS) $N_L(E_F^L) \approx m_{eLFS} p_{FLFS} / (2\pi)^2$ exceeds the one on the pocket $N_P(E_F^P) = m_{eP} p_{FP} / (2\pi)^2$ by the factor $p_{FLFS} / p_{FP} \approx 1$. Therefore the change in the temperature of the transition $T_C - T_{C0}$ as a function of pressure is simply proportional to the DOS on the pocket. Assume the first-order transition takes place at $P_{cr} \approx 123$ GPa. T_C changes from $T_C \approx 100$ K to $T_C \approx 200$ K²⁻⁴ with the pocket emerging simultaneously with the onset of the cubic *Im-3m* phase. A decrease in T_C after the high- T_C phase onset, according to (10), signifies *shrinking* of the pocket size p_{FP} with applying higher pressure. This interpretation is in contrast with the scenario¹⁷ of the pockets developing via the Lifshitz 2.5- topological transition as in that case the pockets sizes would *grow* with pressure.

Discussion and Summary. From a survey of *ab initio* calculations we conclude that the accuracy of state-of-art first-principles methods is insufficient to identify unambiguously the character of the thermodynamic transition between the high- and low- T_C phase of H_3S .

We provide arguments that a first-order order phase transition, possibly related to an instability at a finite structural vector, is the most credible concept to account for a step-like increase of T_C at $P_{cr} \approx 123 \text{ GPa}$ ⁴. We also demonstrate that the decrease in T_C in the high- T_C phase that immediately follows the first-order order transition and the maximum point of $T_{C,max} \approx 203 \text{ K}$ signifies that hole-like pockets emerge simultaneously with the transition into the high- T_C phase.

The strong rise of T_C from $\approx 100 \text{ K}$ in the low- T_C phase to $\approx 200 \text{ K}$ in the high- T_C phase is attributed to the *pre-vailing* contribution to pairing by high-frequency hydrogen modes over that by the acoustic modes. In the low- T_C phase the two phonons groups contribute to T_C almost equally.

Our analysis points out that methods of calculating T_C based on the McMillan extrapolation, successful for ordinary superconductors, are not applicable to H_3S because of its complex phonons spectrum comprised of acoustic and several optical hydrogen modes with much higher frequency. The proposed modification for describing pairing on large Fermi surfaces provides realistic values for the temperature of the onset of superconductivity. The calculated isotopic dependence of T_C turns out to be different on the two sides of the transition, in agreement with^{3,4}.

Comparing the contributions to T_C from the large part of the Fermi surface and from a pocket we conclude that superconductivity in H_3S is driven by interactions on the former. We point out that the presence of small pockets in the high- T_C phase can be revealed by the detection of *two* superconducting gaps in the tunneling spectra of H_3S at low temperatures.

The main results can be summarized as follows.

- A first-order phase transition is the most credible concept accounting for the step-like increase of T_C at $P_{cr} \approx 123 \text{ GPa}$ observed in⁴.
- The usual methods of calculating T_C being inapplicable to H_3S because of its complex phonons spectrum, we have formulated a modified approach to the full scheme of pairing on large Fermi surfaces. The method is based on separating the contributions of optical and acoustic phonons. It provides realistic values for the superconducting transition temperature and allows us to analyze the relative contributions of the phonon branches (“coupling distribution”).
- The isotope dependence of T_C (i.e., its change produced by the deuterium-hydrogen substitution) is evaluated and turns out to be different on the two sides of the transition, in agreement with experiments^{3,4}.
- A microscopic explanation is provided for the unusual behavior of T_C in the high- T_C phase, namely its decrease with increasing pressure. This irregular behavior of T_C above $T_{C,max}$ is ascribed to the presence of small hole-like pockets.
- The contributions to pairing and to the magnitude of T_C from the large part of the Fermi surface and that from a pocket are compared. We conclude that superconductivity in H_3S is driven by pairing on the former.
- The presence of small pockets in the high- T_C phase leads to the appearance of two superconducting gaps in the energy spectrum of H_3S ; this can be revealed via tunneling experiments.

References

1. N. W. Ashcroft. Metallic hydrogen: A high-temperature superconductor? *Phys. Rev. Lett.* **21**, 1748 (1968).
2. A. P. Drozdov, M. I. Erements & I. A. Troyan. Conventional superconductivity at 190 K at high pressures. arXiv:1412.0460 (2014).
3. A. P. Drozdov, M. I. Erements, I. A. Troyan, V. Ksenofontov & S. I. Shylin. Conventional superconductivity at 203 Kelvin at high pressures in the sulfur hydride system. *Nature* **525**, 73 (2015).
4. M. Einaga *et al.* Crystal Structure of 200 K-Superconducting Phase of Sulfur Hydride System. arXiv: 1509.03156 v1 (2015).
5. Y. Li, J. Hao, H. Liu, Y. Li & Y. Ma. The metallization and superconductivity of dense hydrogen sulfide. *J. Chem. Phys.* **140**, 174712 (2014).
6. D. Duan *et al.* Pressure-induced metallization of dense (H₂S)₂H₂ with high-T_c superconductivity. *Sci. Rep.* **4**, 6968 (2014).
7. D. Duan *et al.* Pressure induced decomposition of solid hydrogen sulfide. *Phys. Rev. B* **91**, 180502 (2015).
8. Y. Li *et al.* Dissociation products and structures of solid H₃S at strong compression. *Phys. Rev. B* **93**, 020103 (2016).
9. N. Bernstein, C. S. Hellberg, M. D. Johannes, I. I. Mazin & M. J. Mehl. What superconducts in sulfur hydrides under pressure and why. *Phys. Rev. B* **91**, 060511 (R) (2015).
10. D. Papaconstantopoulos, B. Klein, M. Mehl & W. Pickett. Cubic H₃S around 200 GPa: An Atomic hydrogen superconductor stabilized by sulfur. *Phys. Rev. B* **91**, 184511 (2015).
11. J. A. Flores-Livas, A. Sanna & E. K. U. Gross. High temperature superconductivity in sulfur and selenium hydrides at high pressure. *Euro.Phys. J. B* **89**, 63 (2016).
12. I. Errea *et al.* High-Pressure Hydrogen Sulfide from First Principles: A Strongly anharmonic phonon-mediated superconductor. *Phys. Rev. Lett.* **114**, 157004 (2015).
13. I. Errea *et al.* Quantum hydrogen bond symmetrization and high-temperature superconductivity in hydrogen sulfur system. *Nature* **532**, 81 (2016).
14. E. Nicol & J. Carbotte. Comparison of pressurized sulfur hydride with conventional superconductors. *Phys. Rev. B* **91**, 220507 (2015).
15. R. Akashi, M. Kawamura, S. Tsuneyuki, Y. Nomura & R. Arita. First principles study of the pressure and crystal structure dependence of the superconducting transition temperature in compressed sulfur hydrides. *Phys. Rev. B* **91**, 224513 (2015).
16. C. Neil & L. Boeri. Influence of bonding on superconductivity in high-pressure hydrides. *Phys. Rev. B* **92**, 06058 (2015).
17. A. Bianconi & T. Jarlborg. Lifshitz transitions and zero point lattice fluctuations in sulfur hydride showing near room temperature superconductivity. *Novel Superconducting Materials* **1**, 15 (2015).
18. T. Jarlborg & A. Bianconi. Breakdown of the Migdal approximation at Lifshitz transitions with a giant zero-point motion in H₃S superconductor. arXiv: 1509.07451 (2015).
19. A. Bianconi & T. Jarlborg. Superconductivity above the lowest Earth temperature in pressurized sulfur hydride. *Europhys. Lett.* **112**, 37001 (2015).
20. A. Durajski, R. Szczesniak & Y. Li. Non-BCS properties of H₃S superconductor. *Phys. C* **515**, 1 (2015).
21. A. Durajski, R. Szczesniak & L. Pietronero. High-temperature study of superconducting hydrogen and deuterium sulfide. *Ann. Phys. (Berlin)* **1** (2015).

22. Y. Quan & W. Pickett. van Hove singularities and spectral smearing in high temperature superconducting H₃S. *Phys. Rev. B* **93**, 104526 (2016).
23. R. Akashi, W. Sano, R. Arita & R. Tsuneyuki. Possible Magneli phases and self-alloying in the superconducting sulfur hydride. arXiv:1512.06680 (2015).
24. W. Sano, T. Korenune, T. Tadano, R. Akashi & R. Arita. Effect of van Hove singularities on high T_c superconductivity in H₃S. *Phys. Rev. B* **93**, 094525 (2016).
25. A. B. Migdal. Interaction between electrons and lattice vibrations in a normal metal. *JETP* **7**, 996 (1958).
26. G. M. Eliashberg. Interaction between electrons and lattice vibrations in a superconductor. *JETP* **11**, 696 (1960).
27. I. M. Lifshits. Anomalies of electron characteristics of a metal in the high pressure region. *JETP* **11**, 1130 (1960).
28. Y. Blanter, M. Kaganov, A. Pantsulaya & A. Varlamov. The theory of electronic topological transitions. *Phys. Rep.* **245**, 159 (1994).
29. L. P. Gor'kov. On the energy spectrum of superconductors. *JETP* **7**, 505 (1958).
30. A. A. Abrikosov, L. P. Gor'kov & I. E. Dzyaloshinskii. *Methods of Quantum Field Theory in Statistical Physics*, Dover, NY (1975).
31. W. L. McMillan & J. M. Rowell In *Superconductivity*. v. 1 (Ed. Parks, R. D.) Ch. 11, 561–614 (Marcel Dekker, 1969).
32. E. Wolf. *Principles of Electron Tunneling Spectroscopy* (Oxford Press, 2012).
33. G. Grimvall. *The Electron-Phonon Interaction in Metals* (North-Holland, 1981).
34. B. Geilikman, V. Kresin & N. Masharov. Transition temperature and energy gap for superconductors with strong coupling. *J. Low Temp. Phys.* **18**, 241 (1975).
35. P. Allen & R. Dynes. Transition temperature of strong-coupled superconductors reanalyzed. *Phys. Rev. B* **12**, 905 (1975).
36. J. Carbotte. Properties of Boson-exchange superconductors. *Rev. Mod. Phys.* **62**, 1027 (1990).
37. W. McMillan. Transition temperature of strong-coupled superconductors. *Phys. Rev.* **167**, 331 (1968).
38. R. Dynes. McMillan equation and the T_c of superconductors. *Solid State Comm.* **10**, 615 (1972).
39. N. Zavaritskii, E. Itskevich & A. Voronovskii. Effect of pressure on lattice oscillations and electron-phonon interaction in superconductors. *JETP* **33**, 762 (1971).
40. H. Wang, J. Tse, K. Tanaka, T. Litaka & Y. Ma. Superconductive sodalite-like clathrate calcium hydride at high pressures. *PNAS* **109**, 6463 (2012).
41. L. Landau & E. Lifshits. *Statistical Physics*. v.1 (Elsevier, 1980).
42. L. Landau & E. Lifshits. *Quantum Mechanics* (Pergamon Press, 1977).
43. V. Kresin & B. Kokotov. Dispersion law and structural transitions in crystalline films. *JETP* **48**, 537 (1978).
44. C. Varma & A. L. Simons. Strong coupling theory of charge-density wave transitions. *Phys. Rev. Lett.* **51**, 138 (1983).
45. L. Gor'kov & G. Gruner. In *Charge Density Waves* Ch. 1, 1–14 (North-Holland, 1989).
46. W. L. McMillan. Landau Theory of charge-density waves in transition-metal dichalcogenides. *Phys. Rev. B* **12**, 1187 (1975).
47. L. P. Gor'kov. Superconducting transition temperature: Interacting Fermi gas and phonon Mechanisms in the nonadiabatic regime. *Phys. Rev. B* **93**, 054517 (2016).

Acknowledgements

The authors thank M.I. Eremets for clarification of a number of significant experimental details and providing us with more useful literature references and to M. Calandra for stimulating discussions and sharing some of his theoretical results before publication. The work of LPG is supported by the National High Magnetic Field Laboratory through NSF Grant No. DMR-1157490, the State of Florida and the U.S. Department of Energy. The work of VZK is supported by the Lawrence Berkeley National Laboratory, University of California at Berkeley, and the U.S. Department of Energy.

Author Contributions

L.P.G. and V.Z.K. conceived the project together, V.Z.K. prepared the sections on T_c and the isotope effect, L.P.G. prepared the sections on the phase sequence and transition thermodynamics, the remaining sections and the final version of the manuscript were prepared jointly.

Additional Information

Supplementary information accompanies this paper at <http://www.nature.com/srep>

Competing financial interests: The authors declare no competing financial interests.

How to cite this article: Gor'kov, L. P. and Kresin, V. Z. Pressure and high-T_c superconductivity in sulfur hydrides. *Sci. Rep.* **6**, 25608; doi: 10.1038/srep25608 (2016).



This work is licensed under a Creative Commons Attribution 4.0 International License. The images or other third party material in this article are included in the article's Creative Commons license, unless indicated otherwise in the credit line; if the material is not included under the Creative Commons license, users will need to obtain permission from the license holder to reproduce the material. To view a copy of this license, visit <http://creativecommons.org/licenses/by/4.0/>